ACS Catalysis

Research Article

pubs.acs.org/acscatalysis

When Weaker Can Be Tougher: The Role of Oxidation State (I) in P- vs N-Ligand-Derived Ni-Catalyzed Trifluoromethylthiolation of Aryl Halides

Indrek Kalvet,[†] Qianqian Guo,[‡] Graham J. Tizzard,[§] and Franziska Schoenebeck*[,†]

[†]Institute of Organic Chemistry, RWTH Aachen University, Landoltweg 1, 52074 Aachen, Germany

[‡]Institute of Inorganic Chemistry, X-ray Crystallography, RWTH Aachen University, Landoltweg 1, 52074 Aachen, Germany

[§]EPSRC National Crystallography Service, School of Chemistry, University of Southampton, University Road, SO17 1BJ Southampton, United Kingdom

Supporting Information

ABSTRACT: The direct introduction of the valuable SCF_3 moiety into organic molecules has received considerable attention. While it can be achieved successfully for aryl chlorides under catalysis with $Ni^0(cod)_2$ and dppf, this report investigates the Ni-catalyzed functionalization of the seemingly more reactive aryl halides ArI and ArBr. Counterintuitively, the observed conversion triggered by dppf/Ni^0 is ArCl > ArBr > ArI, at odds with bond strength preferences. By a combined computational and experimental approach, the origin of this was identified to be due to the formation of (dppf)Ni^I, which favors β-F elimination as a competing pathway over the productive cross-coupling, ultimately generating the inactive complex (dppf)Ni(SCF_2) as a catalysis dead end. The complexes (dppf)Ni^I–Br and (dppf)Ni^I–I were isolated and resolved by X-ray crystallography. Their formation was found to be consistent with a ligand-exchange-induced comproportionation mechanism. In stark contrast to these phosphine-derived Ni complexes, the corresponding nitrogen-ligand-derived species were found to be likely competent catalysts in oxidation state I. Our computational studies of N-ligand derived Ni^I complexes fully support productive Ni^I/Ni^{III} catalysis, as the competing β-F elimination is disfavored. Moreover, N-derived Ni^I complexes are predicted to be more reactive than their Ni^0 counterparts in catalysis. These data showcase fundamentally different roles of Ni^I in carbon–heteroatom bond formation depending on the ligand sphere.

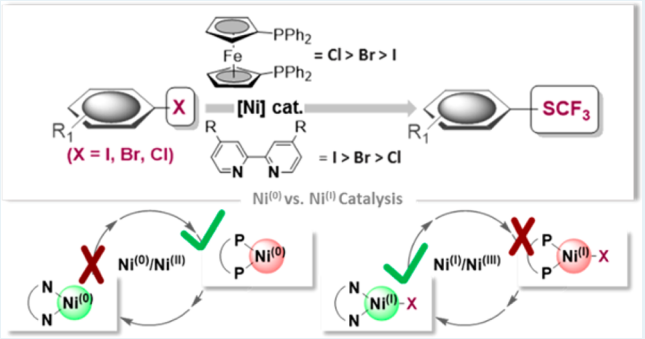

KEYWORDS: *nickel, cross-coupling, DFT, fluorine, mechanisms, ligand*

INTRODUCTION

The past decade has seen numerous impressive advances in the area of homogeneous nickel catalysis.[1] The limits of the oxidative addition step have continuously been pushed back to some of the least activated bonds, such as the recent breakthrough of aryl ether functionalizations, for example.[2,3] In addition, nickel catalysis features a rich mechanistic portfolio, which ranges from the ability to more readily interchange among oxidation states 0, I, II, and III to the possibility for electron transfer processes (Figure 1) in cross-coupling.[4] While capitalization on these diverse mechanistic possibilities has allowed the development of rich and novel synthetic organic chemistry in recent years, the very same mechanistic diversity also poses challenges in achieving the desired key features of modern and sustainable catalytic transformation: e.g. efficiency, low catalyst loading, recyclability, catalyst robustness, generality in substrate, and high functional group tolerance. To achieve high efficiency and generality, catalyst deactivation processes and side reactions will need to be overcome. This in turn requires a fundamental understanding of their origins. In this context, the role and potential catalytic competence of the odd oxidation state I has been questioned.[5,6]

Interestingly, while Ni^I species derived from N ligands have been postulated as catalytically competent intermediates in alkyl–alkyl couplings, e.g. in recent photoredox applications as well as in cross-coupling reactions of challenging electrophiles,[6] for phosphine-ligand-derived Ni^I complexes, there are limited mechanistic data available. The latter complexes have been observed in reactions that employed Ni^0 as catalyst but suggested to be catalytically inactive[7,8] or reported to be less active than Ni^0.[9] On the other hand, Martin recently presented detailed mechanistic data supporting Ni^I as an active species in the activation of C–OMe bonds.[10] Matsubara[11a] and Louie[11b] observed activities in Kumada and Suzuki couplings with NHC-

Received: November 25, 2016
Revised: January 27, 2017
Published: January 31, 2017

DOI: 10.1021/acscatal.6b03344
ACS Catal. 2017, 7, 2126–2132

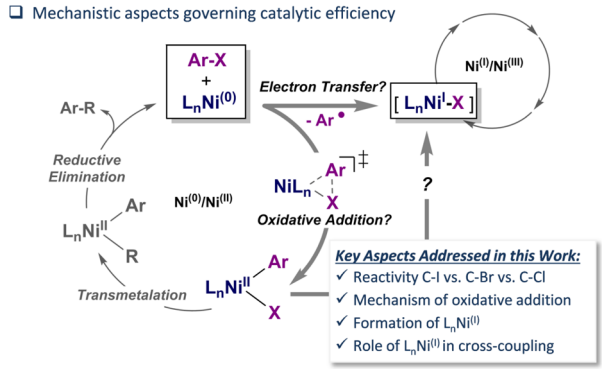

Figure 1. Key features and challenges of Ni catalysis.

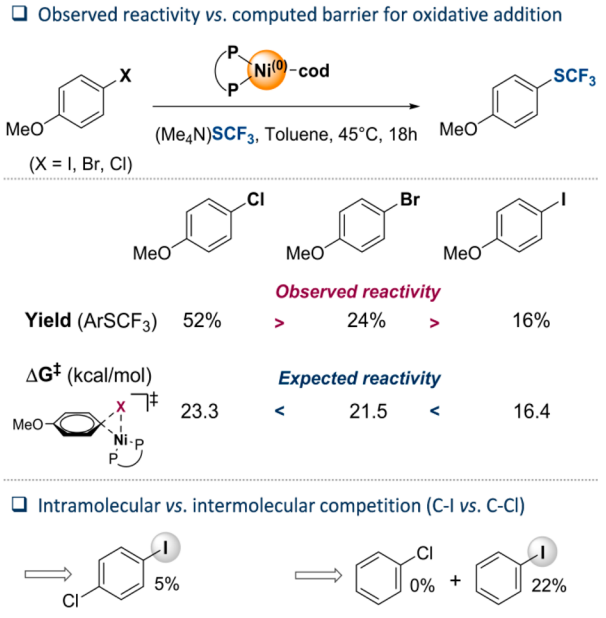

Figure 2. Observed reactivity order (C−Cl > C−Br > C−I) in the dppf/Ni^0(cod)$_2$-catalyzed trifluoromethylthiolation, at odds with the computed barriers.

bound Ni^I complexes. To shine a light on these contrasting observations, we undertook a combined computational and experimental study of the nickel-catalyzed trifluoromethylthiolation reactions of aryl halides as a case study.

Access to ArSCF$_3$ compounds is of pharmaceutical and agrochemical significance due to their associated advantageous lipophilicity properties.[12] Direct catalytic access is of particular interest.[13,14] Aryl iodides and bromides can be converted to ArSCF$_3$ via Pd^0 [15] and Pd^I−Pd^I catalysis with (Me$_4$N)SCF$_3$ or alternative nucleophilic SCF$_3$ sources.[16] In the context of Ni catalysis, Vicic has shown that a Ni(cod)$_2$/bipyridine[17] system allows for functionalization of aryl iodides and selected bromides, but not aryl chlorides. These in turn can be transformed with a phosphine-based catalyst system, Ni(cod)$_2$/dppf, that forms [(dppf)Ni^0(cod)] in situ.[7,18]

In this report, we will show that [(dppf)Ni^0(cod)], in contrast to a bipyridine-derived Ni catalyst, counterintuitively leads to much lower conversions for those aryl halides that have weaker bonds: i.e., aryl iodides and bromides. We will unravel this reactivity behavior herein, unambiguously assigning the role of Ni^I for P- vs N-derived ligands in trifluoromethylthiolation, and uncover the pathways of their origins.

RESULTS AND DISCUSSION

We started our investigations with the systematic comparison of the efficiency of C−SCF$_3$ bond formation of 4-methoxy-substituted aryl halides in toluene at 45 °C with (Me$_4$N)SCF$_3$ under Ni(cod)$_2$/dppf (10 mol %) catalysis conditions. While 4-chloroanisole was converted to the corresponding ArSCF$_3$ in 52% yield, the generally more reactive aryl bromide gave only a 24% yield and the corresponding iodide as little as 16% of the trifluoromethylthiolated product (see Figure 2). These reactivities are at odds with the expected intrinsic ease of the aryl halides toward oxidative addition by a [Ni^0] catalyst, as reinforced by the computed activation barriers of oxidative addition (see Figure 2). Our calculations at the M06L level of theory[19] showed that the barrier to oxidatively add an aryl iodide to [(dppf)Ni^0(cod)] is 7 kcal/mol lower in energy than that of the seemingly more reactive aryl chloride.

To assess the inherent preference for C−SCF$_3$ bond formation in greater detail, we subsequently undertook *intra*- and *inter*molecular competition experiments (C−I vs C−Cl), with Figure 2 presenting the results. While the selectivity followed the expected ease of oxidative addition, showing exclusive functionalization of the C−I site, the overall conversion to product was low (5% for intramolecular and 22% for intermolecular competition). Thus, the lower yields obtained in the reactions with the weaker C−halogen bond substrates do not correlate with the intrinsic reactivities toward oxidative addition but instead must arise from alternative factors that render the catalysis nonproductive.

To gain deeper insight, we performed ^{19}F and ^{31}P NMR spectroscopic analyses of the reaction mixtures after 15 h. These indicated that the characteristic signals of [(dppf)-Ni^0(cod)] had disappeared, and instead a new species had formed that gives two triplets in the ^{31}P NMR (resonating at 30.8 ppm (J = 23.0 Hz) and at 22.1 ppm (J = 37.6 Hz)) and a dd in the ^{19}F NMR spectrum (at −44.8 ppm (J = 37.6, 23.0 Hz)). While we had observed this species also in our previous studies,[20] we had not previously been able to assign its structure or explain its origin. However, we now succeeded in the isolation and characterization of single crystals, unambiguously confirming that the thiocarbonyl-bound [Ni^0] complex **1** was formed (Figure 3). Attempts to react ArI, ArBr, and ArCl with

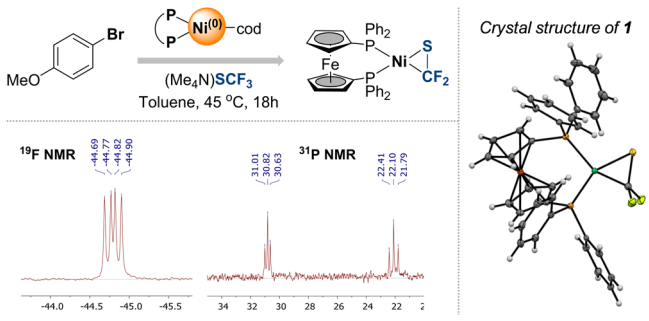

Figure 3. Deactivation of Ni^0 to **1** occurring under catalytic conditions.

(Me$_4$N)SCF$_3$ and complex **1** showed no reaction, suggesting that **1** was catalytically inactive and therefore a product of catalyst deactivation.[20] Computational analysis further indicates that the S=CF$_2$ ligand is very strongly bound to the Ni center—ligand exchange with 1,5-cyclooctadiene is predicted to be endothermic by 21.3 kcal/mol.[19]

DOI: 10.1021/acscatal.6b03344
ACS Catal. 2017, 7, 2126−2132

Species **1** could in principle arise from the trapping of a potential decomposition side product ($F_2C{=}S$) of the employed $(Me_4N)SCF_3$ reagent by the $[Ni^0]$ catalyst.[21] However, our separate subjection of $(Me_4N)SCF_3$ to $Ni(cod)_2$/dppf at 45 °C indicated that this would be unlikely, as **1** was not formed. Moreover, there was no indication of the formation of $F_2C{=}S$ in solution, as judged by ^{19}F NMR analysis. Instead, **1** is likely derived directly from an alternative Ni intermediate.

Given the formal loss of a fluorine atom, a β-fluoride elimination step is mechanistically required. Literature precedence suggests that β-fluoride elimination from $[Ni^{II}]$ intermediates would be feasible.[22] Thus, to gain insight whether the likely origin of **1** is a $[Ni^{II}]$ or an alternative Ni species, we computationally investigated the ease of β-F elimination from $[(dppf)Ni^{II}(SCF_3)(Ph)]$ relative to the productive reductive elimination pathway (Figure 4). Our data, obtained at the CPCM(toluene)M06/def2TZVP//ωB97XD/6-31G(d)(SDD) level of theory suggests β-F elimination is disfavored by $\Delta\Delta G^{\ddagger}$ = 7.5 kcal/mol.[23]

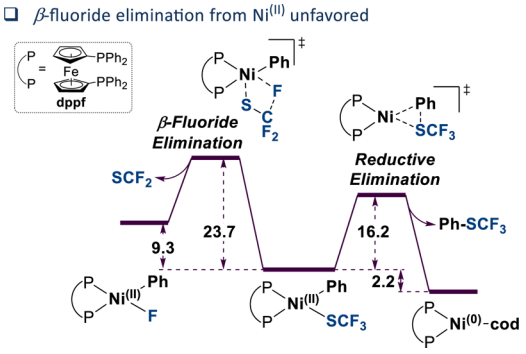

Figure 4. Computational comparison of β-F elimination and reductive elimination pathways from Ni^{II}. Shown are the $\Delta\Delta G^{\ddagger}$ values in kcal/mol, calculated at the CPCM(toluene)M06/def2TZVP//ωB97XD/6-31G(d)(SDD) level of theory.[23]

In line with these calculations are the following experimental observations: while subjection of the product $ArSCF_3$ to $Ni(cod)_2$/dppf will eventually give rise to the deactivation complex **1**, this process occurs on a slower time scale in comparison to that observed for the forward reactions.[24] Moreover, given the higher propensity for subsequent oxidative addition of the liberated $[Ni^0]$ to either ArI or ArBr (in comparison to ArCl) upon reductive elimination of $ArSCF_3$ under catalysis conditions, the unproductive reverse reaction with the product, $ArSCF_3$, can also be ruled out as the predominant cause of the catalysis dead end **1** for the weaker versus stronger C–halogen bond electrophiles.[25]

We speculated that the initial oxidative addition step may be the cause of the divergent reactivities. Thus, we subsequently monitored the oxidative addition of $[(dppf)Ni^0(cod)]$ to ArI, ArBr, and ArCl in the absence of $(Me_4N)SCF_3$. We observed that in all cases a paramagnetic species was formed, which we could unambiguously assign as $[Ni^I]$ upon X-ray crystallographic analyses. While the oxidative addition to ArCl[7] and ArBr give the tricoordinate monomer $[(dppf)Ni^I\text{-}X]$, interestingly, for the iodide, a dimer is the favored species in the solid state (see Figure 4).[26,27] The observed relative ease of the formation of $[Ni^I]$ follows the order ArI > ArBr > ArCl.

These data are in line with the pioneering and seminal studies by Kochi on the oxidative addition of $Ni^0(PEt_3)_4$ to aryl halides.[28] Kochi proposed an electron transfer mechanism as origin of $[Ni^I]$. However, we detected the formation of biaryl products in all cases, suggesting that a different mechanism for the formation of $[Ni^I]$ may be operative. As an alternative for the electron transfer mechanism there have been reports on $[Ni^I]$ formation via ligand exchanges on a $[Ni^{II}]$ intermediate.[11]

As illustrated in Figure 5, following the oxidative addition of $[Ni^0]$ to ArX, ligand exchange from $[(dppf)Ni^{II}(X)(Ph)]$ to

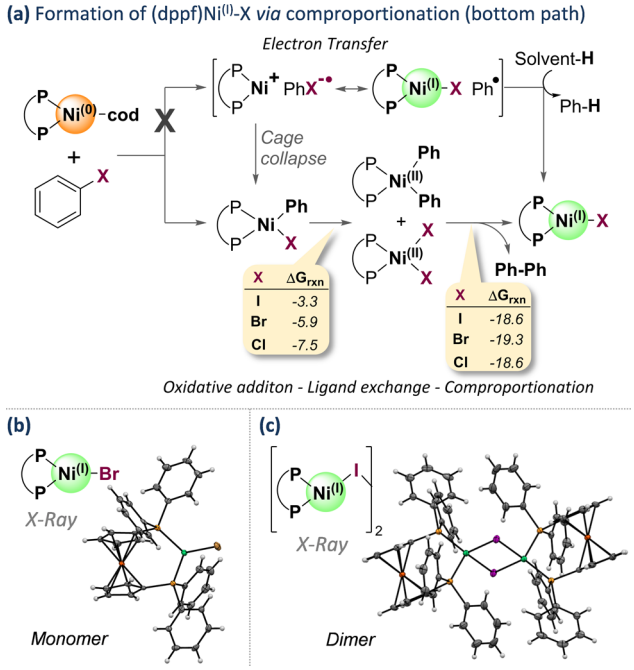

Figure 5. Likely mechanism of $[Ni^I]$ formation and calculated free energy changes (in kcal/mol) of the ligand exchange and reductive elimination + comproportionation steps (a) and crystal structures of $(dppf)Ni^I$ bromide (b) and iodide (c).[19f,27]

$[(dppf)Ni^{II}(X)_2]$ and $[(dppf)Ni^{II}(Ph)_2]$ may likely occur, followed by reductive elimination of biaryl from $[Ni^{II}]$ and subsequent comproportionation of the resulting $[Ni^0]$ with $[Ni^{II}]$ (see Figure 5).[29] The formation of $[(dppf)Ni^{II}X_2]$ as an intermediate was also unambiguously confirmed through its isolation (in addition to Ni^I) and characterization (via ^1H NMR and X-ray crystallography) from the reaction of Ni^0 and PhI in benzene.[30] Our computational data indicate that the ligand exchange step from $[(dppf)Ni^{II}(X)(Ph)]$ to $[(dppf)Ni^{II}X_2]$ and $[(dppf)Ni^{II}(Ph)_2]$ is favorable, being exergonic for all halides (ΔG = −7.5, −5.9, and −3.3 kcal/mol for X = Cl, Br, I, respectively; see Figure 5). Subsequent reductive elimination of biphenyl and formation of $[(dppf)Ni^0(cod)]$ is also thermodynamically favored (by 17.1 kcal/mol). Finally, comproportionation of $[(dppf)Ni^{II}X_2]$ and $[(dppf)Ni^0(cod)]$ is also exergonic for all halides, with ΔG = −1.5, −2.2, and −1.5 kcal/mol for X = Cl, Br, I, respectively (relative to the Ni^{II} and Ni^0 complexes). As such, the steps leading from $[(dppf)Ni^{II}(Ph)(X)]$ to $[Ni^I]$ are thermodynamically favored (see Figure 5).

Would the $[Ni^I]$ species that we observed ultimately generate complex **1**, leading to a catalysis dead end, or perhaps remain a competent species for the generation of $ArSCF_3$? To test this, we initially subjected $(Me_4N)SCF_3$ to $[(dppf)Ni^I(Cl)]$. This

DOI: 10.1021/acscatal.6b03344
ACS Catal. 2017, 7, 2126–2132

led to rapid formation of the deactivated thiocarbonyl-bound [Ni^0] complex **1**, as judged by ^{19}F NMR analysis, suggesting that if any [(dppf)$Ni^I(SCF_3)$] species were to be generated upon halogen to SCF_3 exchange, facile β-fluoride elimination would take place (Figure 6). In line with this, our calculations

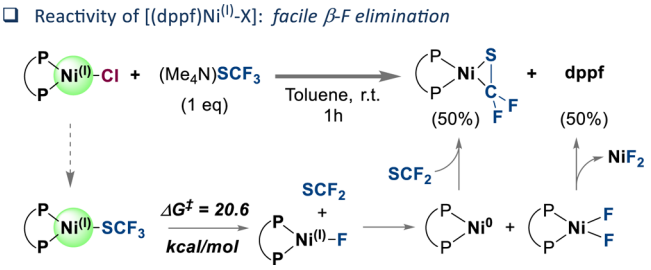

Figure 6. Facile reactivity of [Ni^I] to form **1** (P-P = dppf).

of the β-F elimination from [(dppf)$Ni^I(SCF_3)$] predicted that this process is relatively facile ($\Delta G^{\ddagger}$ = 20.6 kcal/mol). The thereby generated [(dppf)$Ni^I(F)$] complex could subsequently undergo disproportionation to generate [(dppf)$Ni^{II}(F)_2$] and [Ni^0]. The latter would ultimately trap S=CF_2 to give **1** (Figure 6). Consistent with this mechanism, our quantitative ^{31}P NMR spectroscopic analysis of the reaction mixture of $(Me_4N)SCF_3$ with [(dppf)Ni^I(Cl)] indicated that after 1 h ~50% of the employed [(dppf)Ni^I(Cl)] was converted to [(dppf)$Ni^0(SCF_2)$] **1** (and ~50% free dppf was also formed[31]).

The transition states of β-fluoride elimination from Ni^I (panel (a)) and Ni^{II} (panel (b)) complexes are illustrated in Figure 7. The TS derived from Ni^I is slightly later, as expressed

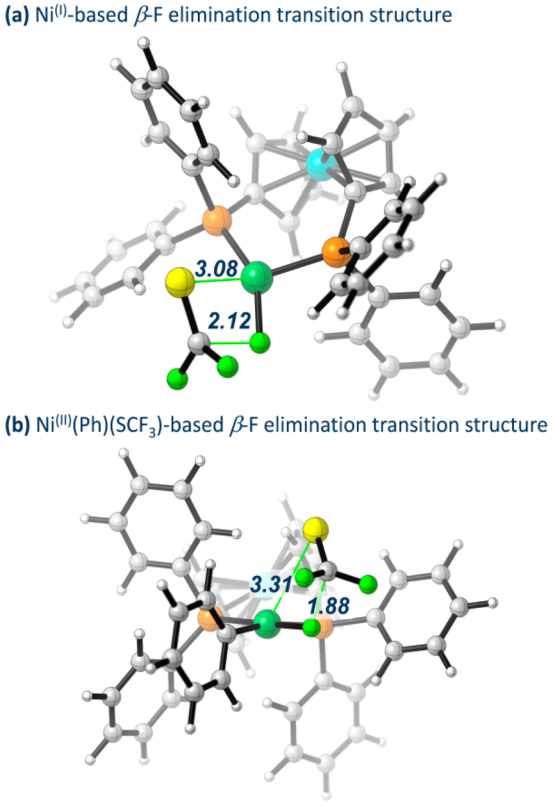

Figure 7. Calculated β-F elimination transition state structures from Ni^I (a) and Ni^{II} (b), shown with the Ni−S and C−F distances (in Å).

by the longer C−F distance (2.12 Å for Ni^I and 1.88 Å for Ni^{II}). This suggests a greater stabilization in the TS derived from Ni^I, which is reflected also in the shorter Ni−S distance in case of Ni^I (3.08 Å for Ni^I vs 3.31 Å for Ni^{II}) as well as the presence of a free coordination site.[23]

These results are a clear indicator that [(dppf)Ni^ISCF_3] is a competent and very potent source of the catalytically inactive complex **1**.[32] The generation of [Ni^I] therefore is detrimental to trifluoromethylthiolation. The origin of lower conversions of aryl iodides and aryl bromides in comparison to the generally less reactive aryl chlorides can be unambiguously correlated to their relative propensity to form [Ni^I]. The key to productive catalysis in (dppf)Ni^0-derived catalysis is therefore a low concentration of the [(dppf)Ni^{II}(X)(Ar)] intermediate that is formed upon oxidative addition to prevent ligand exchanges, as well as a rapid transmetalation and follow-up reaction. Transmetalation generally follows M^{II}−Cl > M^{II}−Br > M^{II}−I (for M = Pd, Ni),[33] paralleling the observed efficiencies of C−SCF_3 bond formation.

Many powerful Ni-catalyzed synthetic methods employ N-derived ligands, such as pyridine derivatives, instead of the otherwise more donating P-based ligands. In line with this, Vicic and co-workers elegantly showed that Ni(cod)$_2$ along with dmbpy (=4,4′-dimethoxybipyridine) as a ligand results in the trifluoromethylthiolation of aryl iodides and certain bromides, but not chlorides.[17] In light of our above observations with P-derived Ni^0, there hence appear to be fundamental reactivity differences between N- and P-coordinated Ni catalysts. Given that N-derived ligands led to the opposite reactivity (X = I, efficient; X = Cl, no conversion), this implies that for N-based ligands either the formation of Ni^I is suppressed or the competing β-F elimination is no longer favorable, therefore avoiding catalyst deactivation products.

We thus also computationally assessed the dmbpy/Ni(cod)$_2$-catalyzed trifluoromethylthiolation of aryl iodides.[35] The obtained data suggest that, in stark contrast to Ni^0/dppf, the corresponding Ni^0/dmbpy system does not proceed via Ni^0/Ni^{II} catalysis but instead by Ni^I/Ni^{III} (see Figure 8). Interestingly, the Ni^0/Ni^{II} catalytic cycle is disfavored primarily due to a high-barrier reductive elimination step of $ArSCF_3$ from [(dmbpy)$Ni^{II}(SCF_3)$(Ph)] ($\Delta G^{\ddagger}$ = 33.1 kcal/mol). In contrast, a Ni^I/Ni^{III} pathway is characterized by much lower activation free energy barriers of 12.9 kcal/mol for oxidative addition and 16.1 kcal/mol for reductive elimination (Figure 8b). These data also agree with previous studies highlighting facile oxidative addition to (N-N)Ni^I complexes.[6h,34]

Moreover, the corresponding β-F elimination from [(dmbpy)$Ni^I(SCF_3)$] is significantly less favored ($\Delta G^{\ddagger}$ = 23.6 kcal/mol) than the productive pathway: oxidative addition of [(dmbpy)Ni^ISCF_3] to ArI occurs preferentially ($\Delta\Delta G^{\ddagger}$=10.7 kcal/mol). While the β-F eliminations are comparable in magnitude for N- and P-derived Ni^I species, the N-based system is overall more effective, as the barriers for the productive Ni^I/Ni^{III} pathway are significantly lower. In comparison, the direct oxidative addition of iodobenzene to [(dppf)$Ni^I(SCF_3)$] is calculated to proceed with a barrier of 32.8 kcal/mol, being significantly greater ($\Delta\Delta G^{\ddagger}$ = 12.2 kcal/mol) than the barrier of the competing β-F elimination pathway. The observed trends are likely related to the different steric properties of the dmbpy and dppf ligands. The smaller bipyridine ligand would still allow facile oxidative addition to the tricoordinate Ni^I-SCF_3, while the lack of steric bulk would stabilize the Ni^{II} species and thus not allow facile reductive

DOI: 10.1021/acscatal.6b03344
ACS Catal. 2017, 7, 2126−2132

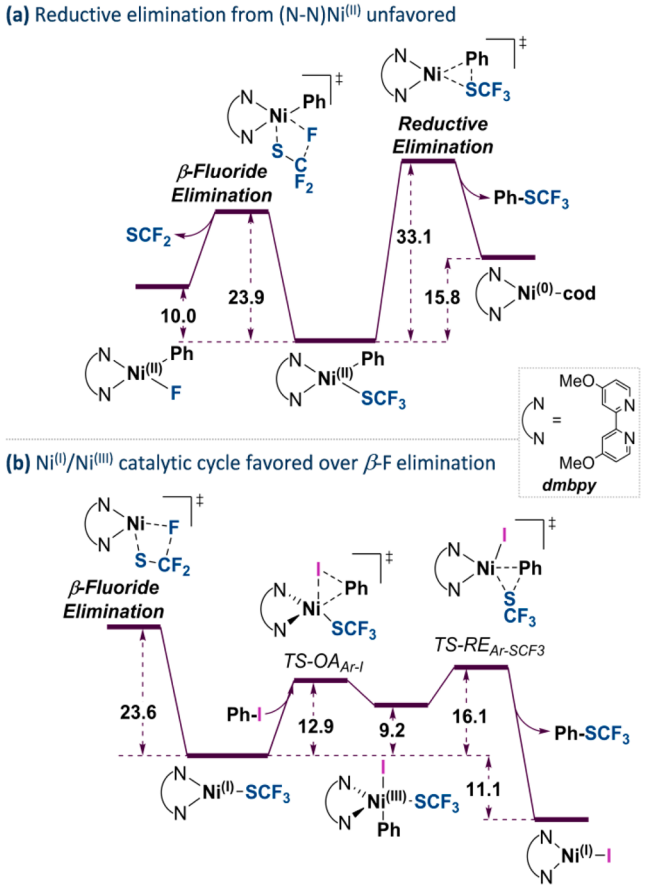

Figure 8. (a) Computational comparison of β-F-elimination and reductive elimination pathways with dmbpy-ligated Ni^{II}. (b) Ni^{I}/Ni^{III} catalytic cycle being favored over β-F elimination.

elimination. With dppf, on the other hand, the steric bulk of the phenyl groups readily allows reductive elimination from Ni^{II} but hampers oxidative addition to Ni^{I}.

Overall, these data strongly indicate that (dppf)Ni^{I} primarily is a less competent catalyst than (dppf)Ni^{0}, as it suffers from a relatively high oxidative addition barrier to ArX, which renders the competing β-F elimination favored, ultimately giving the catalytically inactive complex **1**. In stark contrast, bipyridine-ligand-derived Ni^{I} shows much lower barriers for productive catalysis, rendering the competing processes disfavored. The β-F elimination therefore has served as a mechanistic probe to differentiate between the divergent reactivities of the various plausible oxidation states (0, I, and II) as a function of ligand, using a combination of experiments and computation. Such unambiguous differentiations are otherwise challenging to accomplish.

CONCLUSIONS

In summary, using a combination of computational and experimental studies, we examined the key factors for efficiency in C–SCF_3 bond formation, catalyzed by phosphine- and nitrogen-based nickel complexes. Our data show that, for dppf, [Ni^{I}] species may readily form with the relative ease ArI > ArBr > ArCl under typical [Ni^{0}] catalysis conditions. This will be detrimental for the agrochemically and pharmaceutically relevant C–SCF_3 bond formation, as the corresponding [(dppf)Ni^{I}-SCF_3] undergoes facile β-fluoride elimination more readily over productive catalysis, leading to [(dppf)-$Ni^{0}(SCF_2)$] complex **1**, which is catalytically incompetent and a catalysis dead end. Our mechanistic data support that [(dppf)Ni^{I}] is derived from Ni^{II} precursors via a comproportionation mechanism under concomitant formation of biaryl, not through reductive electron transfer pathways. The reverse was observed for the nitrogen-based Ni/dmbpy system: the corresponding [Ni^{I}] species promotes efficient Ni^{I}/Ni^{III} catalysis, rendering unproductive β-F elimination from Ni^{I} disfavored. In contrast, a Ni^{0}/Ni^{II} cycle suffers from high activation barriers at the elementary steps (oxidative addition and reductive elimination) with bipyridine as ligand. These data highlight the prerequisites for selective Ni-catalyzed couplings of aryl halides and showcase the potential and reactivity of Ni^{I} as a catalyst for different ligands. Our future efforts are directed at exploring the full potential of catalysis at Ni^{I}.

ASSOCIATED CONTENT

Supporting Information

The Supporting Information is available free of charge on the ACS Publications website at DOI: 10.1021/acscatal.6b03344.

Detailed experimental procedures, spectroscopic data, computational details, and energies of computed structures (PDF)
Cartesian coordinates of computed structures (XYZ)
Crystallographic data for **1** (CIF)
Crystallographic data for [(dppf)Ni^{I}Br] (CIF)
Crystallographic data for [(dppf)$Ni^{I}I]_2$ (CIF)
Crystallographic data for [(dppf)$Ni^{II}I_2$] (CIF)

AUTHOR INFORMATION

Corresponding Author

*E-mail for F.S.: franziska.schoenebeck@rwth-aachen.de.

ORCID

Indrek Kalvet: 0000-0002-6610-2857
Franziska Schoenebeck: 0000-0003-0047-0929

Notes

The authors declare no competing financial interest.

ACKNOWLEDGMENTS

We thank the RWTH Aachen, the MIWF NRW, and the European Research Council (ERC-637993) for funding. Calculations were performed with computing resources granted by JARA-HPC from RWTH Aachen University under project "jara0091".

REFERENCES

(1) (a) Johansson Seechurn, C. C. C.; Kitching, M. O.; Colacot, T. J.; Snieckus, V. *Angew. Chem., Int. Ed.* **2012**, *51*, 5062–5085. (b) *Metal-Catalyzed Cross-Coupling Reactions*, 2nd ed.; Wiley-VCH: Weinheim, Germany, 2004. (c) Tamaru, Y., Introductory Guide to Organonickel Chemistry. In *Modern Organonickel Chemistry*; Wiley-VCH: Weinheim, Germany, 2005; pp 1–40.

(2) For reviews, see: (a) Rosen, B. M.; Quasdorf, K. W.; Wilson, D. A.; Zhang, N.; Resmerita, A.-M.; Garg, N. K.; Percec, V. *Chem. Rev.* **2011**, *111*, 1346–1416. (b) Yamaguchi, J.; Muto, K.; Itami, K. *Eur. J. Org. Chem.* **2013**, *2013*, 19–30. (c) Milburn, R. R.; Snieckus, V. *Angew. Chem., Int. Ed.* **2004**, *43*, 888–891. (d) Gavryushin, A.; Kofink, C.; Manolikakes, G.; Knochel, P. *Org. Lett.* **2005**, *7*, 4871–4874. (e) Guan, B.-T.; Wang, Y.; Li, B.-J.; Yu, D.-G.; Shi, Z.-J. *J. Am. Chem. Soc.* **2008**, *130*, 14468–14470. (f) Quasdorf, K. W.; Tian, X.; Garg, N. K. *J. Am. Chem. Soc.* **2008**, *130*, 14422–14423. (g) Ehle, A. R.; Zhou, Q.; Watson, M. P. *Org. Lett.* **2012**, *14*, 1202–1205. (h) Ge, S.; Hartwig, J. F. *Angew. Chem., Int. Ed.* **2012**, *51*, 12837–12841.

DOI: 10.1021/acscatal.6b03344
ACS Catal. 2017, 7, 2126–2132

(3) For Ni-catalyzed functionalization of C−O electrophiles, see: (a) Yu, D.-G.; Li, B.-J.; Shi, Z.-J. *Acc. Chem. Res.* **2010**, *43*, 1486−1495. (b) Muto, K.; Yamaguchi, J.; Lei, A.; Itami, K. *J. Am. Chem. Soc.* **2013**, *135*, 16384−16387. (c) Cornella, J.; Zarate, C.; Martin, R. *Chem. Soc. Rev.* **2014**, *43*, 8081−8097. (d) Tobisu, M.; Chatani, N. *Acc. Chem. Res.* **2015**, *48*, 1717−1726. (e) Dankwardt, J. W. *Angew. Chem., Int. Ed.* **2004**, *43*, 2428−2432. (f) Tobisu, M.; Shimasaki, T.; Chatani, N. *Angew. Chem., Int. Ed.* **2008**, *47*, 4866−4869. (g) Liu, X.; Hsiao, C.-C.; Kalvet, I.; Leiendecker, M.; Guo, L.; Schoenebeck, F.; Rueping, M. *Angew. Chem., Int. Ed.* **2016**, *55*, 6093−6098.

(4) (a) Montgomery, J., Organonickel Chemistry. In *Organometallics in Synthesis*; Wiley: Hoboken, NJ, 2013; pp 319−428. (b) Tasker, S. Z.; Standley, E. A.; Jamison, T. F. *Nature* **2014**, *509*, 299−309. (c) Colon, I.; Kelsey, D. R. *J. Org. Chem.* **1986**, *51*, 2627−2637.

(5) For phosphine ligands, Ni^0/Ni^{II} catalysis is generally assumed. The role of Ni^I is unclear.

(6) For N-type ligands and alkyl−alkyl and alkyl−aryl couplings, Ni^I is assumed to be a catalytic intermediate: (a) Bakac, A.; Espenson, J. H. *J. Am. Chem. Soc.* **1986**, *108*, 719−723. (b) Jones, G. D.; Martin, J. L.; McFarland, C.; Allen, O. R.; Hall, R. E.; Haley, A. D.; Brandon, R. J.; Konovalova, T.; Desrochers, P. J.; Pulay, P.; Vicic, D. A. *J. Am. Chem. Soc.* **2006**, *128*, 13175. (c) Li, Z.; Jiang, Y.-Y.; Fu, Y. *Chem. - Eur. J.* **2012**, *18*, 4345−4357. (d) Powell, D. A.; Maki, T.; Fu, G. C. *J. Am. Chem. Soc.* **2005**, *127*, 510−511. (e) Phapale, V. B.; Buñuel, E.; García-Iglesias, M.; Cárdenas, D. J. *Angew. Chem., Int. Ed.* **2007**, *46*, 8790−8795. (f) Zuo, Z.; Ahneman, D. T.; Chu, L.; Terrett, J. A.; Doyle, A. G.; MacMillan, D. W. C. *Science* **2014**, *345*, 437−440. (g) Weix, D. J. *Acc. Chem. Res.* **2015**, *48*, 1767−1775. (h) Gutierrez, O.; Tellis, J. C.; Primer, D. N.; Molander, G. A.; Kozlowski, M. C. *J. Am. Chem. Soc.* **2015**, *137*, 4896−4899.

(7) Yin, G.; Kalvet, I.; Englert, U.; Schoenebeck, F. *J. Am. Chem. Soc.* **2015**, *137*, 4164−4172.

(8) Ge, S.; Green, R. A.; Hartwig, J. F. *J. Am. Chem. Soc.* **2014**, *136*, 1617−1627.

(9) Guard, L. M.; MohadjerBeromi, M.; Brudvig, G. W.; Hazari, N.; Vinyard, D. J. *Angew. Chem., Int. Ed.* **2015**, *54*, 13352−13356.

(10) Cornella, J.; Gómez-Bengoa, E.; Martin, R. *J. Am. Chem. Soc.* **2013**, *135*, 1997−2009.

(11) Formation of Ni^I from Ni^{II}: (a) Miyazaki, S.; Koga, Y.; Matsumoto, T.; Matsubara, K. *Chem. Commun.* **2010**, *46*, 1932−1934. (b) Zhang, K.; Conda-Sheridan, M.; Cooke, S. R.; Louie, J. *Organometallics* **2011**, *30*, 2546−2552.

(12) (a) Leo, A.; Jow, P. Y. C.; Silipo, C.; Hansch, C. *J. Med. Chem.* **1975**, *18*, 865−868. (b) Hansch, C.; Leo, A.; Taft, R. W. *Chem. Rev.* **1991**, *91*, 165−195.

(13) For reviews of recent advances, see: (a) Xu, X.-H.; Matsuzaki, K.; Shibata, N. *Chem. Rev.* **2015**, *115*, 731−764. (b) Zheng, H.; Huang, Y.; Weng, Z. *Tetrahedron Lett.* **2016**, *57*, 1397−1409.

(14) For selected examples of alternative indirect, electrophilic, or metal-free approaches or examples involving alternative coupling partners (C−H, $C-N_2$,or $C-B(OH)_2$), see: (a) Pooput, C.; Medebielle, M.; Dolbier, W. R. *Org. Lett.* **2004**, *6*, 301−303. (b) Kieltsch, I.; Eisenberger, P.; Togni, A. *Angew. Chem., Int. Ed.* **2007**, *46*, 754−757. (c) Pooput, C.; Dolbier, W. R.; Médebielle, M. *J. Org. Chem.* **2006**, *71*, 3564−3568. (d) Chen, C.; Xie, Y.; Chu, L.; Wang, R.-W.; Zhang, X.; Qing, F.-L. *Angew. Chem., Int. Ed.* **2012**, *51*, 2492−2495. (e) Tran, L. D.; Popov, I.; Daugulis, O. *J. Am. Chem. Soc.* **2012**, *134*, 18237−18240. (f) Shao, X.; Wang, X.; Yang, T.; Lu, L.; Shen, Q. *Angew. Chem., Int. Ed.* **2013**, *52*, 3457−3460. (g) Pluta, R.; Nikolaienko, P.; Rueping, M. *Angew. Chem., Int. Ed.* **2014**, *53*, 1650−1653. (h) Danoun, G.; Bayarmagnai, B.; Gruenberg, M. F.; Goossen, L. J. *Chem. Sci.* **2014**, *5*, 1312−1316. (i) Xu, J.; Mu, X.; Chen, P.; Ye, J.; Liu, G. *Org. Lett.* **2014**, *16*, 3942−3945. (j) Honeker, R.; Ernst, J. B.; Glorius, F. *Chem. - Eur. J.* **2015**, *21*, 8047−8051.

(15) (a) Teverovskiy, G.; Surry, D. S.; Buchwald, S. L. *Angew. Chem., Int. Ed.* **2011**, *50*, 7312−7314. (b) Yin, G.; Kalvet, I.; Schoenebeck, F. *Angew. Chem., Int. Ed.* **2015**, *54*, 6809−6813. (c) Xu, C.; Shen, Q. *Org. Lett.* **2014**, *16*, 2046−2049.

(16) Alternatively, for a method with stoichiometric use of Cu, see: Weng, Z.; He, W.; Chen, C.; Lee, R.; Tan, D.; Lai, Z.; Kong, D.; Yuan, Y.; Huang, K.-W. *Angew. Chem., Int. Ed.* **2013**, *52*, 1548−1552.

(17) Zhang, C.-P.; Vicic, D. A. *J. Am. Chem. Soc.* **2012**, *134*, 183−185.

(18) During the preparation of this paper a Ni-catalyzed directing-group-based approach for the coupling of aryl chlorides was reported: Nguyen, T.; Chiu, W.; Wang, X.; Sattler, M. O.; Love, J. A. *Org. Lett.* **2016**, *18*, 5492−5495.

(19) (a) Calculations performed at the CPCM(toluene)M06L/def2TZVP//ωB97XD/6-31G(d)(SDD) level of theory.. (b) Frisch, M. J.; Trucks, G. W.; Schlegel, H. B.; Scuseria, G. E.; Robb, M. A.; Cheeseman, J. R.; Scalmani, G.; Barone, V.; Mennucci, B.; Petersson, G. A.; Nakatsuji, H.; Caricato, M.; Li, X.; Hratchian, H. P.; Izmaylov, A. F.; Bloino, J.; Zheng, G.; Sonnenberg, J. L.; Hada, M.; Ehara, M.; Toyota, K.; Fukuda, R.; Hasegawa, J.; Ishida, M.; Nakajima, T.; Honda, Y.; Kitao, O.; Nakai, H.; Vreven, T.; Montgomery, J. A., Jr.; Peralta, J. E.; Ogliaro, F.; Bearpark, M.; Heyd, J. J.; Brothers, E.; Kudin, K. N.; Staroverov, V. N.; Kobayashi, R.; Normand, J.; Raghavachari, K.; Rendell, A.; Burant, J. C.; Iyengar, S. S.; Tomasi, J.; Cossi, M.; Rega, N.; Millam, J. M.; Klene, M.; Knox, J. E.; Cross, J. B.; Bakken, V.; Adamo, C.; Jaramillo, J.; Gomperts, R.; Stratmann, R. E.; Yazyev, O.; Austin, A. J.; Cammi, R.; Pomelli, C.; Ochterski, J. W.; Martin, R. L.; Morokuma, K.; Zakrzewski, V. G.; Voth, G. A.; Salvador, P.; Dannenberg, J. J.; Dapprich, S.; Daniels, A. D.; Farkas, Ö.; Foresman, J. B.; Ortiz, J. V.; Cioslowski, J.; Fox, D. J. *Gaussian 09, Revision D.01*; Gaussian, Inc., Wallingford, CT, 2013. For the appropriateness of the chosen computational method, see: (c) Sperger, T.; Sanhueza, I. A.; Kalvet, I.; Schoenebeck, F. *Chem. Rev.* **2015**, *115*, 9532−9586. For synergistic studies employing computation and experiment, see: (d) Tsang, A. S. K.; Sanhueza, I. A.; Schoenebeck, F. *Chem. - Eur. J.* **2014**, *20*, 16432−16441. (e) Sperger, T.; Sanhueza, I. A.; Schoenebeck, F. *Acc. Chem. Res.* **2016**, *49*, 1311−1319. (f) We also performed comparisons between M06L and other methods for energy evaluations, such as M06, PBE0-D3, and B3LYP-D3, and found all to give qualitatively the same trends in reactivities and preferred reaction pathways. For optimizations, we found the geometries resulting from ωB97XD to reproduce the crystal structures well..

(20) Dürr, A. B.; Yin, G.; Kalvet, I.; Napoly, F.; Schoenebeck, F. *Chem. Sci.* **2016**, *7*, 1076−1081.

(21) (a) Tavener, S. J.; Adams, D. J.; Clark, J. H. *J. Fluorine Chem.* **1999**, *95*, 171−176. (b) Liu, J.-B.; Xu, X.-H.; Chen, Z.-H.; Qing, F.-L. *Angew. Chem., Int. Ed.* **2015**, *54*, 897−900. (c) Baert, F.; Colomb, J.; Billard, T. *Angew. Chem., Int. Ed.* **2012**, *51*, 10382−10385.

(22) For β-fluoride elimination from Ni^{II}, see: (a) Ichitsuka, T.; Fujita, T.; Arita, T.; Ichikawa, J. *Angew. Chem., Int. Ed.* **2014**, *53*, 7564−7568. (b) Ichitsuka, T.; Fujita, T.; Ichikawa, J. *ACS Catal.* **2015**, *5*, 5947−5950. (c) Fujita, T.; Arita, T.; Ichitsuka, T.; Ichikawa, J. *Dalton Trans.* **2015**, *44*, 19460−19463. For DFT studies on β-fluoride elimination with Pd, see: (d) Zhao, H.; Ariafard, A.; Lin, Z. *Organometallics* **2006**, *25*, 812−819.

(23) We also investigated the potential of alternative mechanisms being at play, such as a phosphine participation in the C−F activation, in analogy to: Nova, A.; Reinhold, M.; Perutz, R. N.; Macgregor, S. A.; McGrady, J. E. *Organometallics* **2010**, *29*, 1824−1831. During the optimization of this TS, however, it collapsed back to our reported TS geometry, where the F atom is transferred directly to the Ni atom.

(24) Similarly, our attempts to "transmetalate" (Cl/SCF_3 exchange) [(dppf)Ni^{II}(Cl)(*o*-tolyl)] to [(dppf)Ni^{II}(SCF_3)(*o*-tolyl)] also eventually formed the thiocarbonyl-bound species **1** (see Figure 3).

(25) The [(dppf)Ni^{II}(SCF_3)(Ar)] intermediate could also undergo ligand exchange to produce [(dppf)Ni^{II}(SCF_3)$_2$] and [(dppf)Ni^{II}(Ar)$_2$]. Upon reductive elimination of Ar-Ar, comproportionation of Ni^0 and Ni^{II} could take place to form a "Ni^I-SCF_3" species which may then undergo the chemistry described in the article to give **1**. While this alternative explains the formation of **1** from $ArSCF_3$, it does not explain the different reactivities observed, ArI < ArBr < ArCl, which is the focus of the discussion.

(26) The complexes were recrystallized from different solvents ([Ni^I-Br] from benzene and [Ni^I-I] from THF).

DOI: 10.1021/acscatal.6b03344
ACS Catal. 2017, 7, 2126−2132

(27) Our calculations of the spin density in the (dppf)Ni^{I}Br complex indicate that the unpaired electron is localized predominantly on the Ni center, suggesting that it is a Ni^{I} complex. Furthermore, we also compared the C−Fe distances in the ferrocene moieties of the obtained crystal structures with the corresponding distances in Fe^{II} (CCDC 1154857) and Fe^{III} (CCDC 194434, 170258, 138350, and 1194362) ferrocenes. The data indicate that our Ni^{I} complexes are more similar to Fe^{II} ferrocene, indicating that there is no substantial electronic exchange between the ferrocene and the Ni center. See the Supporting Information for further information.
(28) Morrell, D. G.; Kochi, J. K. *J. Am. Chem. Soc.* **1975**, *97*, 7262−7270.
(29) For feasibility of comproportionation of Ni^{0} and Ni^{II}, see: (a) Velian, A.; Lin, S.; Miller, A. J. M.; Day, M. W.; Agapie, T. *J. Am. Chem. Soc.* **2010**, *132*, 6296−6297. (b) Beck, R.; Shoshani, M.; Krasinkiewicz, J.; Hatnean, J. A.; Johnson, S. A. *Dalton Trans.* **2013**, *42*, 1461−1475.
(30) It is likely that Ni^{II} precipitated from the reaction mixture due to its poor solubility in benzene. A single crystal grown from benzene/hexane yielded the Ni^{II} species, while from THF/hexane crystals of the Ni^{I} species were obtained.
(31) The formation of **1** was initially accompanied by the appearance of a dark red precipitate, which ultimately (after ∼1 h) turned bright green, and free dppf could then be detected by ^{31}P NMR spectroscopic analysis. The free dppf may originate from the initially formed (dppf)NiF_2, since our attempts to independently prepare (dppf)NiF_2 from dppf and NiF_2 turned out to be unsuccessful, as indicated by the lack of new signals in paramagnetic ^{1}H NMR and quantitative recovery of free ligand, on the basis of ^{31}P qNMR analysis.
(32) In comparison, it takes more than 24 h at 45 °C to fully convert $PhSCF_3$ + [Ni^{0}] to [$Ni(SCF_2)$].
(33) (a) Casado, A. L.; Espinet, P. *J. Am. Chem. Soc.* **1998**, *120*, 8978−8985. (b) Ariafard, A.; Lin, Z.; Fairlamb, I. J. S. *Organometallics* **2006**, *25*, 5788−5794.
(34) Calculations were performed at the CPCM(THF)M06/def2TZVP//ωB97XD/6-31G(d)(SDD) level of theory.
(35) Phapale, V. B.; Guisán-Ceinos, M.; Buñuel, E.; Cárdenas, D. J. *Chem. - Eur. J.* **2009**, *15*, 12681−12688.

DOI: 10.1021/acscatal.6b03344
ACS Catal. 2017, 7, 2126−2132